Hourly LST Monitoring with the Japanese Geostationary Satellite MTSAT-1R over the Asia-Pacific Region

Kei OYOSHI[1*], Shin AKATSUKA[2], Wataru TAKEUCHI[3] and Shinichi SOBUE[1]

[1]*Earth Observation Research Center, Japan Aerospace Exploration Agency, 2-1-1 Sengen, Tsukuba, Ibaraki, Japan*

[2]*Yamanashi Institute of Environmental Sciences, 5597-1 Kenmarubi, Kamiyoshida, Fujiyoshida, Yamanashi 403-0005, Japan*

[3]*The University of Tokyo, 4-6-1 Komaba, Meguro-ku, Tokyo, 153-8505, Japan*

Abstract

Land Surface Temperature (LST) is a significant indicator of the energy balance at the Earth's surface, and measurements of LST are required for a wide variety of climate, hydrological, ecological, and biogeochemical studies. As LST is temporally highly variable, an hourly LST map enables an improved understanding of the surface energy balances. In this study, hourly LST was estimated from thermal infrared data of the Japanese geostationary satellite, the Multi-functional Transport Satellite-1R (MTSAT-1R). Numerical coefficients of the Generalized Split-Window equations were optimized based on the results of radiative transfer simulations. Model accuracies were less than, or equal to 1.09 K for a viewing zenith angle (VZA) lower than 40˚ and 1.73 K for a VZA of 60˚. Using a comparison of clear-sky images of six different climatic, land cover, and viewing angle regions (Australia, Indonesia, Japan, Mongolia, Papua New Guinea, and Thailand), the RMSE between MTSAT and MODIS LST over these regions was found to range from 2.32 K to 2.86 K, and the bias from -1.22 K to 1.46 K. However, a seasonal stability analysis on a daily basis in 2007 and 2008, demonstrated that consistency largely depends on the amount of cloud in each pair of MTSAT and MODIS LST images. RMSE were within 2 K or 3 K in clear-sky scenes comparison, but worse than 5 K in cloudy scenes. It is therefore considered that to utilize MTSAT LST more effectively and reliably, cloud contamination needs to be assessed, and a precise identification of cloud mask is required to eliminate MTSAT LST with high uncertainties.

Key words: LST, MTSAT, split-window algorithm, radiative transfer simulation, MODIS LST product.

1. Introduction

Land Surface Temperature (LST) is one of the most significant parameters used in understanding the energy balance, snow or ice melt, evapotranspiration, and vegetation growth at the Earth's surface. Hence, LST measurements are required for a wide variety of climate, hydrological, ecological, and biogeochemical studies (Parkinson *et al*., 2000). Until now, LSTs on a continental or global scale have mainly been retrieved using thermal infrared radiation measured by sensors onboard polar-orbiting satellites, such as NOAA Advanced Very High Resolution Radiometer (AVHRR) or Terra/Aqua Moderate Resolution Imaging Spectroradiometer (MODIS) (Price, 1984, Ulivieri *et al*., 1994, Wan *et al*., 1996). However, LST is highly variable temporally and has a large diurnal cycle, and therefore using a temporal resolution of 0.5-1 day is often inadequate for many applications such as numerical weather forecasting, urban heat island monitoring, ecosystem process modeling, or crop growth simulation modeling. Such applications require hourly LSTs or daily min/max/average LSTs for accurate execution. However, geostationary satellites can collect hourly data, and in the case of the Meteosat Second Generation (MSG) Spinning Enhanced Visible Infra-Red Imager (SEVIRI) satellite one image is acquired every 15 min. In addition, the Himawari-8/9 Advanced Himawari Imager (AHI), successor of Multi-functional Transport Satellite (MTSAT) is to be launched in 2014/ 2015, and has

* Corresponding author: ohyoshi.kei@jaxa.jp
Phone: +81-50-3362-7982, Fax: +81-29-868-2961

the capability of acquiring one image every 10 min using 16 bands. Obtaining such hourly LST data would enhance our understanding of thermal conditions at the Earth's surface. Although land-surface monitoring by geostationary satellites has been limited because of poor sensor specifications, recent improvements in this respect have facilitated the use of these sensors, not only for atmospheric monitoring for use in weather forecasts, but also for land-surface monitoring (Fensholt *et al*., 2006). Accordingly, diurnal LST variations can now be retrieved from images obtained by geostationary satellites such as the Geostationary Meteorological Satellite (GMS) (Oku *et al*., 2004, Prata *et al*., 1999), the Geostationary Operational Environmental Satellite (GOES) (Pinker *et al*., 2008), and the MSG satellite (Sobrino *et al*., 2004).

In this study, we present a methodology for use in retrieving hourly LST from the Japanese geostationary satellite MTSAT, which covers the western Asia-Pacific area. Figure 1 shows the framework for use in retrieving LST from MTSAT. Our methodology progresses as follows: firstly, a split-window algorithm for polar-orbiting satellites data was optimized for the MTSAT sensor, and was based on at-sensor measurements of radiative transfer simulations. The optimized split-window algorithm was then used to estimate LST over six selected Asia-Pacific regions from thermal infrared data obtained from MTSAT, and from emissivity data of MODIS LST products. Finally, MTSAT LST products were compared with MODIS LST products, and the usefulness of hourly LST monitoring with MTSAT was demonstrated.

2. Methodology

2.1 Data and Study Area

MTSAT-1R is a Japanese geostationary satellite that was launched on February 26, 2005, and although it has been non-operative since 2011 it remains in standby mode. It covered the Asia-Pacific region from 35,800 km above the equator at 140 degrees east longitude, and obtained images every thirty minutes for the northern hemisphere (once an hour for a full-disk image) in five spectral bands including one visible band with spatial resolutions of 1 km, and four infrared bands with resolutions of 4 km. MTSAT-2 which carries a similar sensor to MTSAT-1R is now currently in operation at 145 degrees of east longitude. In this research, we use the full-disk imagery of MTSAT-1R. Table 1 lists the sensor specifications of MTSAT-1R.

MTSAT-1R uses five spectral bands, including two thermal infrared bands (IR1 and IR2) which are applicable for the estimation of LST. The spatial resolution of the MTSAT

Table 1. Characteristics of the MTSAT-1R sensor.

Band	Wavelength (μm)	Spatial Res. (km)
VIS	0.55 - 0.90	1
IR1	10.3 - 11.3	4
IR2	11.5 - 12.5	4
IR3	6.5 - 7.0	4
IR4	3.5 – 4.0	4

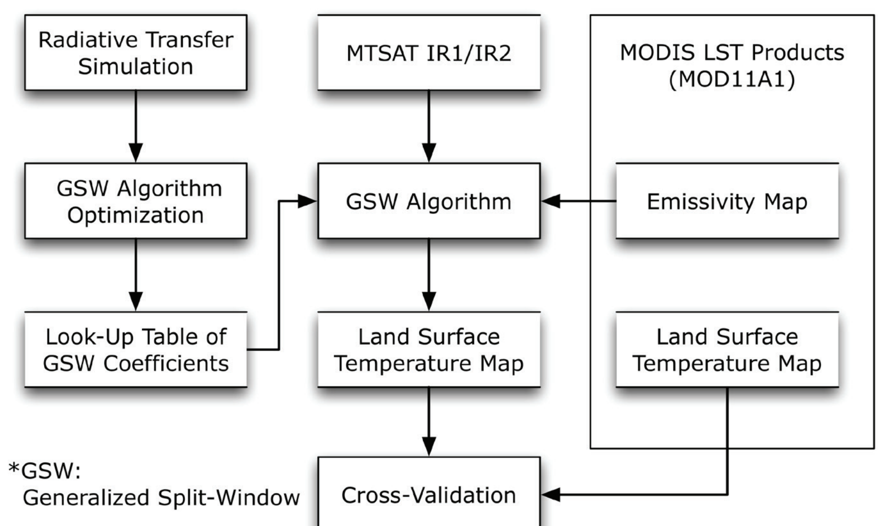

Figure 1. Framework for LST retrieval from MTSAT IR1/IR2 data. The coefficients of generalized split-window (GSW) equation were optimized by using the result of a radiative transfer simulation. The LST was then retrieved from MTSAT IR1/IR2 data and MODIS emissivity products with the GSW equation. Finally, MTSAT LST products were compared with MODIS LST products.

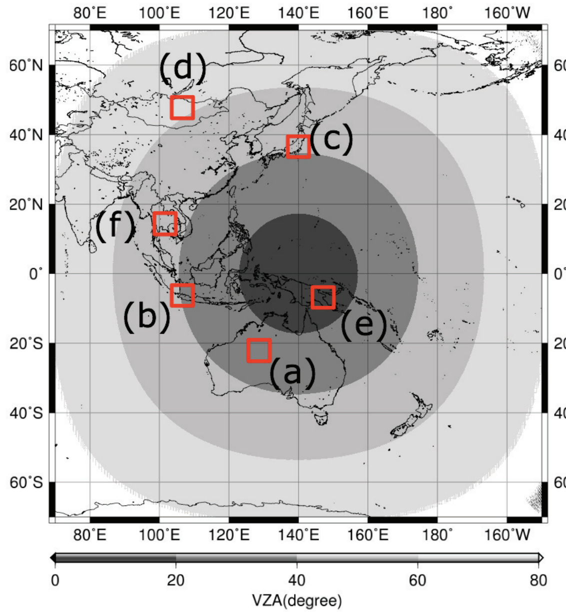

Figure 2. MTSAT-1R field of view and viewing angle, and the location of six study areas: (a) Australia, (b) Indonesia, (c) Japan, (d) Mongolia, (e) Papua New Guinea, and (f) Thailand.

instrument varies with the spectral band, and ranges from 1 km to 4 km at nadir, and although it is coarse compared to polar orbiting satellites it has an excellent temporal resolution (tens of minutes to one hour). In this research, we obtained MTSAT IR1 and IR2 data from Institute of Industrial Science, University of Tokyo. All utilized data were radiometrically calibrated to brightness temperature (K), and geometrically converted to the Plate Carree projection (Takeuchi *et al*., 2010).

Six regions in Australia, Indonesia, Japan, Mongolia, Papua New Guinea, and Thailand, which are all located in different climate zones with differing land cover (including desert, tropical forest, croplands, urban, and grassland areas) and contain widespread viewing zenith angle (VZA) areas, were selected as study areas to confirm the spatial robustness of the proposed methodology. Figure 2 illustrates the MTSAT-1R field of view and VZA, and the six study areas. Table 2 lists the location and approximate VZA of each study area.

2.2 LST Retrieval with Split-Window Algorithm

Atmospheric absorption and emission causes a large difference between the brightness temperatures measured in-situ and those measured by satellite. Therefore, in order to retrieve accurate LST from thermal infrared data provided by satellite measurements, attenuation caused by the interaction between radiation from the Earth's surface and atmospheric contents (mainly water vapor) requires elimination. Many researchers have previously developed algorithms for LST retrieval, and the split-window algorithm using two thermal infrared bands in the 10.5 to12.5 µm wavelength have been widely used (Price, 1984, Sobrino *et al*., 2000, Ulivieri *et al*., 1994), as this algorithm utilizes the differences in water vapor absorption between 11 µm and 12 µm to eliminate the effect of water vapor. Prata *et al*. (1999) used a GMS-5 Visible and Infrared Spin Scan Radiometer (VISSR) to retrieve LSTs, and found that the accuracy validated against ground measurement obtained from two Australian sites was approximately 2-3 K. Sobrino *et al*. (2004) optimized a two-channel algorithm for a European geostationary satellite, namely MSG SEVIRI (Spinning Enhanced Visible and Infrared Imager), and the theoretical accuracy in LST estimation was found to be lower than 1.5 K for VZAs lower than 50˚. However, the algorithm developed by Sobrino *et al*. (2004) requires column water vapor for LST retrieval, and there are currently no available water vapor products able to fulfill the temporal resolution (hourly) and spatial resolution (1-4 km) required for MTSAT data. Pinker *et al*. (2008) evaluated LST from GOES data with various algorithms for LST retrieval and found the accuracy to be about 1-3 K compared with six ground station data located in the United States.

The Generalized Split-Window (GSW) algorithm was originally developed by Wan *et al*. (1996) for retrieving LST from AVHRR and MODIS data, and was modified from the split-window algorithm developed by Becker *et al*. (1990) by optimizing coefficients with the VZA, atmospheric water vapor, and lower boundary temperature. Wan *et al*. (1996) reported that the GSW algorithm was able to estimate LST from MODIS thermal infrared data with an accuracy of less

Table 2. Selected study areas: name, location, and viewing zenith angle (VZA) of MTSAT-1R.

Area	Upper Left	Lower Right	VZA (deg)
Australia	4S, 125E	9S, 130E	20-30
Indonesia	4S, 104E	9S, 109E	30-40
Japan	39N, 137E	34N, 142E	30-40
Mongolia	50N, 104E	45N, 109E	60-70
Papua New Guinea	4S, 143E	9S, 148E	10-20
Thailand	17N, 98E	12N, 103E	40-50

than 1 K for the full range of VZAs across the swath (up to 55° from nadir). As MTSAT is a geostationary satellite, it has a large variety of VZAs; hence, the GSW algorithm is suitable for MTSAT because this algorithm has robustness for VZA variation. In this study, we therefore applied the GSW algorithm to MTSAT data. The GSW equation for MTSAT data is expressed as:

where LST is land surface temperature (K), *IR1* and *IR2* are

$$LST = (a_1 + a_2 \frac{1-\varepsilon}{\varepsilon} + a_3 \frac{\Delta\varepsilon}{\varepsilon^2}) \frac{IR1 + IR2}{2} + (b_1 + b_2 \frac{1-\varepsilon}{\varepsilon} + a_3 \frac{\Delta\varepsilon}{\varepsilon^2}) \frac{IR1 - IR2}{2} + c \quad (1)$$

brightness temperatures (K) of MTSAT IR1 and IR2; and a_i, b_i (i = 1, 2, 3), and c are numerical coefficients. ε_1, ε_2 are surface emissivity of IR1 and IR2; ε and $\Delta\varepsilon$ are defined by $\varepsilon = (\varepsilon_1 + \varepsilon_2)/2$, $\Delta\varepsilon = \varepsilon_1 - \varepsilon_2$, respectively.

Because the coefficients depend greatly on the sensor specifications, the coefficients of the GSW algorithm require optimization for MTSAT. This study therefore also determines coefficients, based on the results of simulated at-sensor measurements, by using the MTSAT Spectral Response Function (SRF). The simulation was implemented by MODTRAN4.3 (Berk *et al*., 2003), which is a widespread radiative transfer code for wavelengths ranging from the visible to the thermal infrared region. At-sensor measurements of MTSAT brightness temperature were simulated under various observational, atmospheric, and land-surface conditions to derive coefficients that were applicable to the entire Asia-Pacific region. Table 3 lists the parameters used in MODTRAN simulations: these ranges were determined based on the previous research of Ouaidrari *et al*. (2002) and Wan (1999). In this study, we performed forward simulations for MTSAT using the conditions from five atmospheric models (tropical, mid-latitude summer/winter, sub-arctic summer/winter) bundled in MODTRAN, with LST ranging from $T_{air}-5$ K to $T_{air}+15$ K, cumulative water vapor (CWV) from 0.5 to 5.0 g/cm^2, emissivity from 0.94 to 1.00, and VZAs from 0 to 60°. T_{air} represents the surface air temperature at the lowest boundary of each atmospheric model. Ouaidrari *et al*. (2002) reported a CWV of 7.0 g/cm^2 in the tropics, although on average it was found to usually vary between 0.3 to 5.5 g/cm^2. Hence the value of 5.0 g/cm^2 was used for the upper value of CWV in this study.

In order to determine the emissivity ranges for the simulation, the band-averaged emissivities of MTSAT IR1 and IR2 bands calculated from representative land-surface materials such as vegetation (dry grass, and the leaves of maple, oak, and pine), water (seawater, distilled water, ice, and snow), soil (soil 90P 476S and Salisbury sample 2535 of Nebraska soil, soil sample 1 of Death Valley soil, and soil sample 1 of Page Arizona Sandy Soil), and man-made materials (black asphalt, cobblestone pavement, and life concrete tile) are shown in Figure 3. The emissivity data were obtained from MODIS UCSB Emissivity Library (http://www.icess.ucsb.

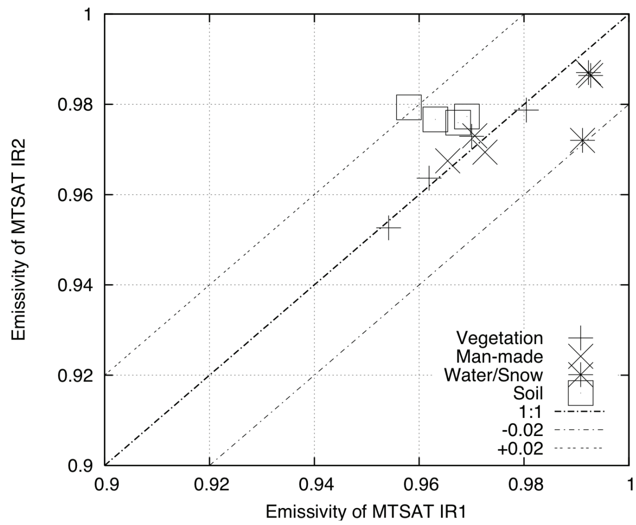

Figure 3. The band-averaged emissivities of MTSAT IR1 and IR2 bands calculated from the emissivities of representative land-surface materials. The middle line represents the 1:1 line. Upper and lower lines indicate that the differences in IR1 and IR2 emissivities are −0.02 and +0.02, respectively.

Table 3. Parameters used in MODTRAN simulations with spectral response function (SRF) of the MTSAT- 1R sensor.

Parameter	Range	Interval
Atmospheric Model	Tropical, Mid-Latitude Summer/Winter	-
	Sub-Arctic Summer/Winter	-
Column Water Vapor (*CWV*)	0.5- 5.0 (g/cm^2)	0.50
Emissivity ε_1, ε_2	0.94 - 1.00	0.02
Viewing Zenith Angle (*VZA)*	0 - 60 (degree)	20
Land Surface Temperature (*LST)*	T_{air}–5 - T_{air}+15 (K)	2

edu/modis/EMIS/html/em.html). The emissivities are distributed from approximately 0.94 to 1.00. In addition, the differences between the IR1 and IR2 emissivities are distributed around the 1:1 line and the absolute values of the differences are almost all less than 0.02. Therefore, we executed the simulations under the conditions that emissivities range from 0.94 to 1.00 and absolute values of the emissivity differences of IR1 and IR2 are less than 0.02.

These conditions were used in the simulation and the results were then used to optimize the numerical coefficients of the GSW algorithm by using the Levenberg-Marquardt algorithm for non-linear minimization. Since the coefficients highly depend on the VZA (Wan *et al*., 1996), the optimized coefficients were calculated for each VZA. We then composed a coefficient look-up table (LUT) with respect to VZAs.

2.3 Emissivity Map

The GSW equation requires the emissivity maps of IR1 and IR2 bands to estimate LST, and the quality of emissivity map strongly affects the accuracies of the LST retrieval. However, land-surface emissivity has high spatial variation and is therefore difficult to estimate, and in addition seasonal changes cause temporal emissivity variations because of alterations in land-surface conditions (in particular, deciduous forest or cropland areas) (Liang, 2004). In this study, the MODIS emissivity map (MOD11A1, collection-5) derived from land cover maps (Snyder *et al*., 1998), MODIS SRF, and emissivity data of various materials were used for the LST retrieval from MTSAT data. However, in order to apply the MODIS emissivity maps to MTSAT LST retrieval, it was necessary to confirm the consistency of the emissivities from the MTSAT and MODIS thermal bands. Therefore, by calculating the average emissivities of MTSAT (IR1, IR2) and MODIS (band31, band32) from the SRFs of two thermal infrared bands, and from the MODIS UCSB Emissivity Library data used in section 2.2, we confirmed that the differences caused by SRF configurations are less than 0.005. According to Wan *et al*. (1996), to achieve an accuracy of 1 K, the uncertainty of the emissivity should be around 0.005, and Snyder *et al*. (1998) used this criterion to evaluate emissivity products. Accordingly, it was found that MODIS emissivity products are applicable to LST retrieval from MTSAT data.

3. Results and Discussions

3.1 Evaluation of Generalized Split-Window Equations Optimized for MTSAT

We firstly evaluated the theoretical accuracies of the derived GSW equations. The numerical coefficients given by Eq. (1) were determined with respect to each VZA. All the coefficients showed statistical significance ($p < 0.05$), and the residual standard errors (RSE) of each VZA are listed in Table 4. The RSE is defined as:

where n is the number of samples; LST is the true LST;

$$RSE = \sqrt{\frac{1}{n-2}\sum_{i=1}^{n}(LST_i - \hat{LST}_i)^2} \qquad (2)$$

and $\hat{LST}$ is the MTSAT LST from the optimized GSW algorithm. RSEs range from 0.86 K to 1.73 K, and tend to increase with the VZA. The slant path length through the atmosphere increases with the VZA, and therefore the simulation results exhibit large variance. However, the derived GSW equations were able to estimate LST with an accuracy of approximately 1 K when the VZA was less than or equal to 40˚, and are thus considered to be acceptable for use with MTSAT LST data for many land applications (Prata *et al*., 1999, Wan *et al*., 1996).

3.2 Comparison with MODIS LST Product

This section examines the results from actual MTSAT data. MTSAT LST was estimated by applying the optimized GSW algorithm with the observed brightness temperatures of MTSAT IR1 and IR2, and MODIS emissivity maps. The GSW coefficients for each VZA were calculated by linear interpolation from the LUT of the GSW coefficients with respect to the VZA (0˚, 20˚, 40˚, and 60˚).

Although validation of MTSAT LST with in-situ measurements is preferable, it is difficult to find spatially homogeneous areas suitable for validating coarse resolution satellite images such as MTSAT data. Even if it was possible, the number of in-situ measurement sites would be limited spatially and temporally. Therefore it would be a practical way to compare with the MODIS LST product, which has been well-validated by in-situ data and an accuracy of more than 1 K has been confirmed in many areas including lakes, grassland, rice fields, and snow covered areas (Wan *et al*., 2002). Furthermore, MODIS LST covers the entire globe on a daily basis. In this study therefore, we confirmed the consistency of MTSAT with MODIS LST MOD11A1 collection-5 product (Wan, 1999). Matchup LST data were observed at almost the same time (at about 10:30 local time) and observation time differences were within 30 minutes. Before the comparison, MODIS LST products were aggregated from 1 km to 4 km of spatial resolution by

Table 4. Theoretical accuracy (Residual Standard Errors) of MTSAT LST estimated by the optimized GSW algorithm for each viewing zenith angle (VZA).

VZA (degree)	RSE (K)
0	0.86
20	0.90
40	1.09
60	1.73

averaging 4 × 4 pixels.

Clear-sky scenes of six Asia-Pacific regions (Australia, Indonesia, Japan, Mongolia, Papua New Guinea, and Thailand) were selected to assess consistency. The MTSAT and MODIS LST maps of the six regions are shown in Figure 4. A visual interpretation showed that the spatial patterns of MTSAT LST were highly consistent with those of MODIS LST. In addition, the LSTs of urban central business district areas such as Tokyo, Jakarta, and Bangkok were found to be higher than those of surrounding areas. As this indicates that MTSTAT LST is able to identify urban heat islands, it can therefore be used to monitor thermal conditions over

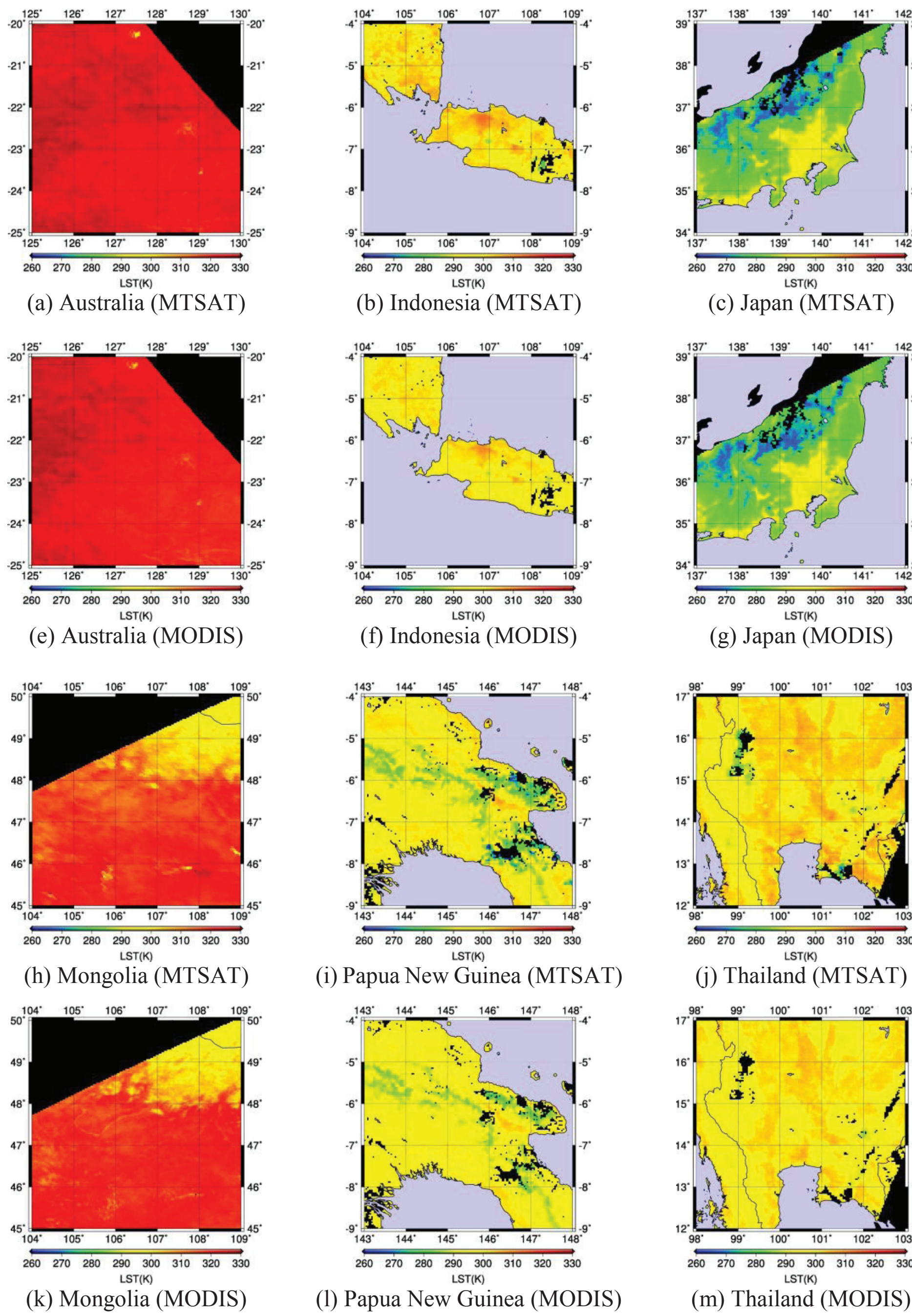

Figure 4. Clear-sky image comparison of MTSAT and MODIS LST over Australia (Nov 15, 2007), Indonesia (Jul 14, 2007), Japan (Mar 1, 2007), Mongolia (Aug 11, 2008), Papua New Guinea (May 25, 2007), and Thailand (Dec 17, 2008). Black pixels represent cloud mask or an area of no data, and were excluded from the comparison.

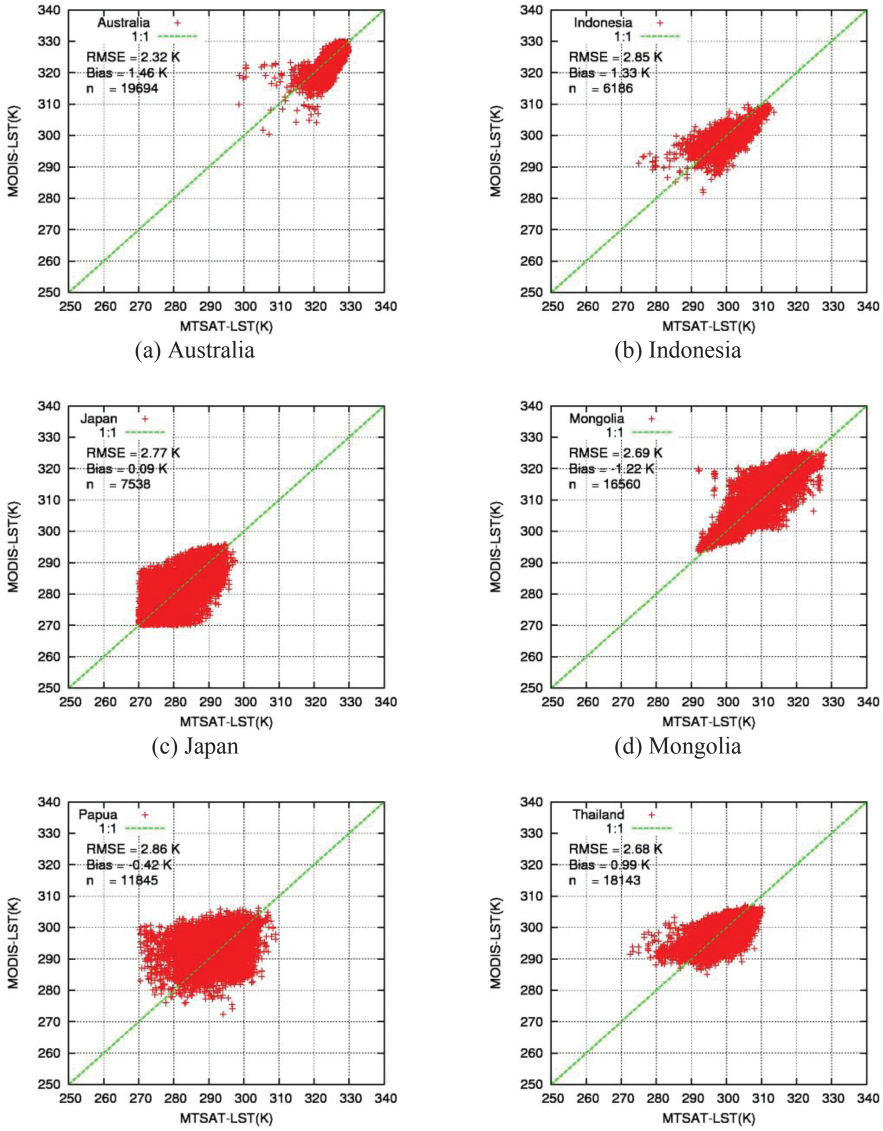

(a) Australia (b) Indonesia

(c) Japan (d) Mongolia

(e) Papua New Guinea (f) Thailand

Figure 5. Scatter plots of MODIS and MTSAT LST, and RMSE, bias, and number of samples over Australia (Nov 15, 2007), Indonesia (Jul 14, 2007), Japan (Mar 1, 2007), Mongolia (Aug 11, 2008), Papua New Guinea (May 25, 2007) and Thailand (Dec 17, 2008).

metropolises on an hourly basis.

Figure 5 illustrates scatter plots and statistics of MODIS and MTSAT LST, including RMSE, bias, and number of samples. The RMSEs of Australia, Indonesia, Japan, Mongolia, Papua New Guinea, and Thailand were 2.32 K, 2.85 K, 2.77 K, 2.69 K, 2.86 K, and 2.68 K, respectively, and the bias ranged from -1.22 K to 1.46 K. In a comparison of clear-sky images, all regions showed a similar consistency with those of MODIS LST, even though these regions differ widely in terms of climate zone, land cover, and VZA.

3.3 Seasonal Stability Assessment of MTSAT LST

The time series stability was assessed using daily LST data observed at approximately 10:30 (local time) throughout 2007 and 2008. Although cloud pixels in the MODIS LST were masked by the MODIS cloud mask product, thin or low altitude clouds remained, and these were difficult for the MODIS spectral data to identify (Ackerman *et al*., 2006). LST cannot be retrieved precisely if the target pixel is obscured by cloud, and we considered that this would be a potential cause of large inconsistencies between MTSAT and MODIS LST. Therefore, to reduce the effect of any remaining cloud, MODIS or MTSAT pixels with a LST lower than 270 K were defined as cloud-obscured pixels and were excluded from comparison. In addition, to mitigate the co-registration error between MOIDS and MTSAT LST images, MTSAT

LST images was shifted to certain offsets on the x and y axes when MTSAT LST was overlaid with MODIS LST to calculate the RMSE or bias. The MTSAT LST image was then moved within ±5 pixels on both the x and y axes, and the offset values were determined when the RMSE between MTSAT and MODIS LST was minimized.

Figure 6 shows daily RMSEs and biases. Temporal profiles of RMSEs and biases in Australia, Japan, and Mongolia indicate large variances and seasonality in one year. In these areas, MTSAT LST was consistent with MODIS LST within 5 K of the RMSE in the dry season, but more than 5 K in the rainy season. For example, Japan showed the RMSE of more than 5 K in the rainy to highly-humid summer season (DOY 150-240), but the RMSE of less than 2-3 K in the dry winter season (DOY 0-60, 330-360). A similar tendency was found in Australia, but in the opposite seasons from those in Japan.

The RMSEs of Australia and Mongolia showed the highest variances among the six regions. Land cover in the study areas of Australia and Mongolia is mostly desert, and the LST therefore changes dramatically over a short time period because the thermal inertia of the desert is high. Therefore, the difference in observation times between MTSAT and MODIS is also considered likely to contribute to inconsistency in desert areas. Furthermore, the quality of MODIS LST can cause inconsistencies: Wan (2013) reported that MODIS LST errors are within ±1 K in most cases, but

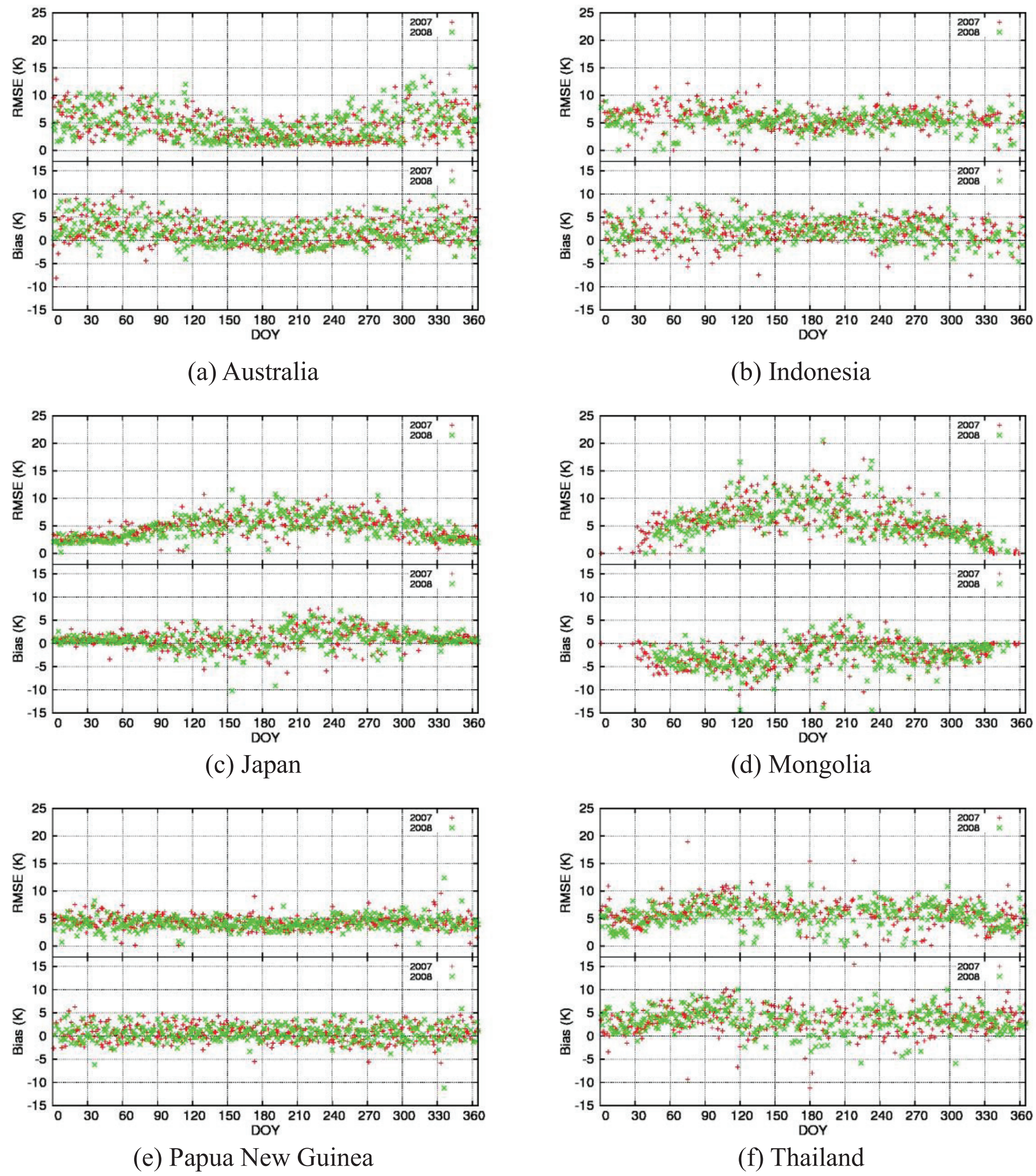

(a) Australia (b) Indonesia

(c) Japan (d) Mongolia

(e) Papua New Guinea (f) Thailand

Figure 6. Daily RMSE and bias between MTSAT and MODIS LST over the six study areas in 2007 and 2008.

more than 2.5 to 4.5 K in desert areas.

In Mongolia, the LST was found to be so low in the winter season that most of the pixels were masked as cloud. There were therefore few comparison results available from this region in winter because a LST lower than 270 K was defined as cloud in this study. The RMSE of Mongolia was the largest among the six study areas, and this is considered to be attributed to both the land cover and the large VZA of 60-70°. Indonesia, Papua New Guinea, and Thailand are located in the tropics, but the RMSE and bias of Papua New Guinea showed a greater stability than the other three study areas. The possible reasons for this are that the VZA is almost nadir (10-20°), and that the land cover of the study area is almost completely forested and therefore has a small temperature variation.

Figure 7 shows the number of clear pixels and RMSE in 2007 and 2008 calculated from daily pair images of MTSAT and MODIS LST, where the RMSE is seen to greatly depend on the number of clear pixels in a scene (the RMSE decreases as the number of clear pixels increases). Although the results of a clear scene comparison in Section 3.2 show a RMSE better than 2-3 K in all regions, at times the cloudy scene comparison indicates an RMSE greater than 5 K. This suggests that the consistency of MTSAT and MODIS LST tends to be dramatically decreased when cloudy image pairs are compared. As cloud pixels remain even with the MODIS cloud mask, a LST thresholding method was applied to eliminate the cloud- obscured pixels. However, the remaining clouds cause a large inconsistency because estimated LST from cloud-obscured pixels is very uncertain. In addition, atmospheric water vapor in a cloudy scene would be higher than that in a clear-sky scene, and large amounts of atmospheric water vapor increase the uncertainty in LST retrieval (Wan, 1999). Moreover, the difference in observation time between MTSAT and MODIS causes a difference in the cloud or water vapor distribution spatially and temporally, and this observation time difference also causes a bias error because LST rises or drops even within 30 minutes. Such cloud and atmospheric-water related factors are the main sources of inconsistency, and the spatio-temporal pattern of these factors results in the inconsistency

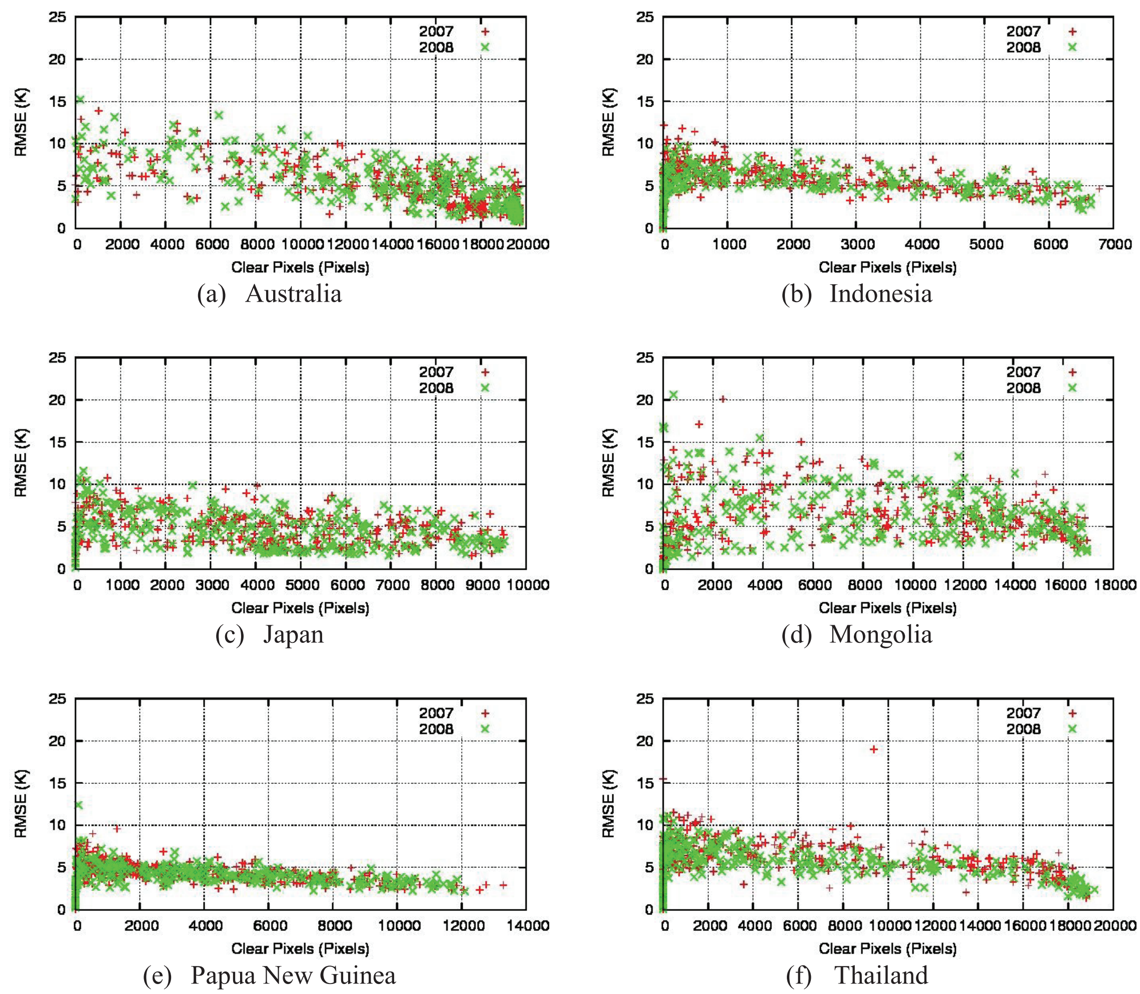

(a) Australia (b) Indonesia (c) Japan (d) Mongolia (e) Papua New Guinea (f) Thailand

Figure 7. The number of clear pixels and RMSE in 2007 and 2008. Each point shows the value calculated from daily pair images of MTSAT and MODIS LST.

of seasonality and locality.

3.4 Hourly LST Observation by MTSAT

Figure 8 shows hourly MTSAT LST and daily MODIS LST (MOD11A1, MYD11A1) observed on March 1, 2007, in central Tokyo, Japan (N35.69˚, E139.76˚), although MODIS LST (MYD11A1) data for the afternoon observation (13:30 JST) was not available because of its poor quality flag. For a comparison, we selected a pixel of MTSAT LST data and aggregated MODIS LST data by averaging 4 × 4 pixels to standardize the pixel size. MTSAT LST was consistent with MODIS LST, but MTSAT was able to capture diurnal changes in greater detail, including minimum, maximum, and inflection points. Such hourly profiles are considered to be useful in gaining a better understanding of energy exchanges between the land and atmosphere.

Finally, monthly composites of hourly MTSAT LST from a full-disk image are shown in Figure 9. Full-disk LST were generated by using the GSW algorithm optimized for MTSAT with monthly global emissivity maps from the MODIS LST product (MOD11C3) to cover the MTSAT full-disk area on a daily basis. Monthly composite images were generated by selecting the pixel with the highest LST from pixels observed at the same hour during August 2007. MTSAT was found to be able to capture the diurnal LST changes over the Asia-Pacific region.

3.5 Discussion

According to literature (Prata *et al*., 1999, Wan *et al*., 1996), RMSEs of 1–3 K are acceptable, accuracies of 1 K are very useful for gaining a better understanding of the entire Earth system on a global scale, and accuracies of 3 K are also useful for limited use. MTSAT LST has an excellent sampling frequency and is considered to be marginally useful for land-surface monitoring, if cloud contamination, atmospheric water vapor, land cover, and VZA are taken into consideration. The accuracy of the LST product from a polar orbiting satellite (POS) like MODIS is better than 1 K in most cases (Wan, 2008). However, LST products from geostationary satellites (including GOES, MSG, or GMS) have been found to have generally an accuracy of between 1 and 3 K (Pinker *et al*., 2008, Prata *et al*., 1999, Sobrino *et al*., 2004), and the results of this study are therefore in agreement with those of previous literature.

The main source of inconsistency is confirmed as being related to remaining clouds, as discussed in Section 3.3. It is therefore considered necessary to evaluate cloud contamination over the target area when MTSAT LST is utilized, and a reliable cloud mask could be quite useful for eliminating MTSAT LST data with high uncertainties. However, in addition to cloud contamination, the optimization of the GSW is considered likely to cause inconsistencies. In this study, the LUT of the GSW coefficients was composed with respect only to VZA, whereas the LUT of the MODIS LST algorithm was composed with respect not only to VZA, but also to atmospheric profiles such as air temperature or atmospheric water vapor. The optimizations of the GSW equations by separating these atmospheric conditions is therefore considered likely to improve the accuracies of the GSW algorithm, although atmospheric profiles are needed to estimate LST. If atmospheric water vapor data is available, a LST retrieval algorithm which directly inputs water vapor to the LST retrieval formula (Sobrino *et al*., 2000) would also be applicable. However, it is difficult to generate a water vapor product that fulfills MTSAT coverage on an hourly basis with a similar spatial resolution.

Other discrepancies are considered to be related to co-registration errors and observation time differences between MTSAT and MODIS, and these differences are inevitable when MODIS LST is used for comparison. Although registration errors were offset by shifting the image on the

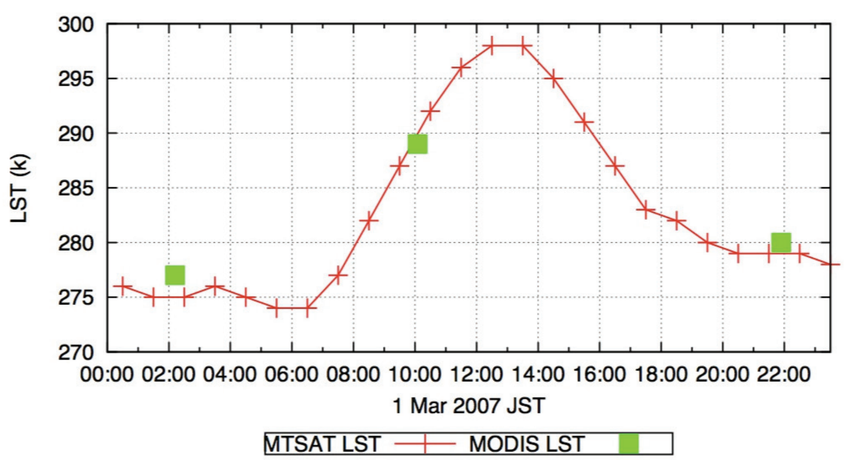

Figure 8. Hourly profile of MTSAT LST and three points of MODIS (MOD11A1, MYD11A1) LST at Tokyo, Japan (Mar 1, 2007, Japan Standard Time). The location of the sampled area in central Tokyo is N35.69˚, E139.76˚.

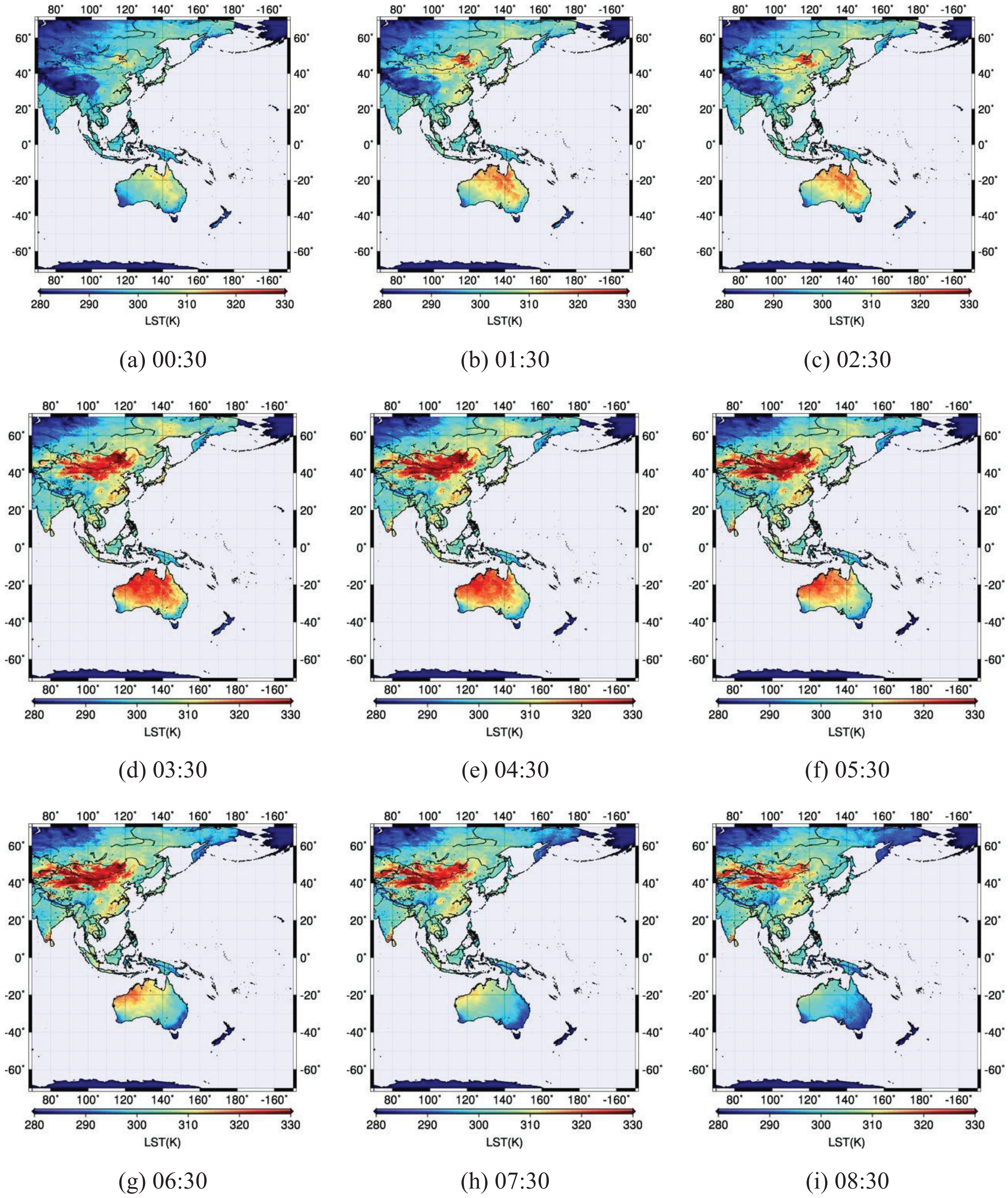

(a) 00:30 (b) 01:30 (c) 02:30

(d) 03:30 (e) 04:30 (f) 05:30

(g) 06:30 (h) 07:30 (i) 08:30

Figure 9. Monthly composite of hourly MTSAT LST (UTC) over the Asia-Pacific region (MTSAT full-disk imagery) in August 2007. The clear-sky images were composited from daily MTSAT LST data of August 2007 to remove cloud contamination.

both x and y axes, non-linear co-registration errors could not be reduced.

Although the model accuracy of MTSAT LST by optimization of the GSW algorithm showed RSEs range from 0.86 K to 1.73 K, the result of a comparison between MTSAT LST data and MODIS LST delivered lower results. It is evident that the above-mentioned factors contribute to inconsistencies, and are largely responsible for the differences between the model accuracy and the actual data comparison result.

Wan (2008) reported that the accuracy of MODIS LST is better than 1 K in most cases, but is worse than 1 K at times, particularly in desert areas. Since the MODIS LST error resulted in inconsistencies, the validation of MTSAT LST against in-situ measurement should be performed in the future, although, as mentioned above, it is difficult to locate a homogeneous area that is suitable for MTSAT LST validation.

In addition, in this study the comparison of daytime data only was assessed, and therefore future studies are required to assess nighttime MTSAT LST stability.

4. Conclusion

We retrieved hourly LST from the thermal infrared data of MTSAT-1R by optimizing the numerical coefficients of the GSW algorithm based on the results of radiative transfer simulations. The model accuracy of the optimized GSW algorithm for MTSAT was found to depend on the viewing zenith angle: 0.86 K at nadir and 1.73 K at 60˚. LST was then estimated from IR1 and IR2 of MTSAT bands using MODIS emissivity maps and the optimized GSW algorithm. MTSAT LST over six Asia-Pacific areas was compared with daytime MODIS LST data. As a result, we found that the spatial patterns of MTSAT LST were highly consistent with those of MODIS LST in clear-sky image comparisons, and RMSE was found to range from 2.32 K to 2.86 K. However, using a comparison of a pair of MTSAT and MODIS LST images, a time-series stability analysis of 2007 and 2008 on a daily basis demonstrated that consistency has a strong correlation with the amount of cloud, where RMSEs were within 2-3 K in clear-sky scenes, but worse than 5 K in cloudy scenes comparison. This resulted in inconsistencies in seasonality or locality between MTSAT and MODIS LST. It is therefore considered that cloud contamination needs to be taken into account in order to utilize MTSAT LST more effectively and reliably, and precise cloud mask is required to eliminate MTSAT LST with a high uncertainty.

Aknowledgements

MODIS data were obtained from the Earth Observing System Clearing House (ECHO) and Warehouse Inventory Search Tool (WIST) at the National Aeronautics and Space Administration (NASA). The authors wish to express their gratitude to anonymous reviewers for providing valuable comments and suggestions.

References

Ackerman, S., Strabala, K., Menzel, P., Fey, R., Moeller, C., Gumley, L., Baum, B., Seemann, S. and Zhang, H. (2006). Discriminating clear-sky from cloud with MODIS Algorithm Theoretical Basis Document (MOD35).

Becker, F. and Li, L. A. (1990). Toward a local split window method over land surface. International Journal of Remote Sensing, 11, 369-393.

Berk, A., Anderson, G. P., Acharya, P. K., Hoke, M. L., Chetwynd, J. H., Bernstein, L. S., Shettle, E. P., Matthew, M. W. and Alder-Golden, S. M. (2003). MODTRAN4 Version 3 Revision 1 User's Manual. Air Force Research Laboratory.

Fensholt, R., Sandholt, I., Stisen, S. and Tucker, C. (2006). Analyzing NDVI for the African continent using the geostationary meteosat second generation SEVIRI sensor. Remote Sensing of Environment, 101, 212-229.

Liang, S. Quantitative Remote Sensing of Land Surfaces. (2004). New Jersey: John Wiley & Sons, Inc., 366-388.

Oku, Y. and Ishikawa, H. (2004). Estimation of land surface temperature over the Tibetan Plateau using GMS data. Journal of Applied Meteorology and Climatology, 48, 548-561.

Ouaidrari, H., Goward, S. N., Czajkowski, K. P., Sobrino, J. A. and Vermote E. (2002). Land surface temperature estimation from AVHRR thermal infrared measurements An assessment for the AVHRR Land Pathfinder II data set. Remote Sensing of Environment, 81, 114-128.

Parkinson, C. L. Greenstone, R. (2000). EOS data products handbook volume 2. NASA Goddard Space Flight Center, 151-154.

Pinker, R. Sun, D., Hung, M. and Li, C. (2008). Evaluation of satellite estimate of land surface temperature from GOES over the United States. Journal of Applied Meteorology and Climatology, 48, 167-180.

Prata, A. J. and Cechet, R. P. (1999) An assessment of the accuracy of land surface temperature determination from the GMS-5 VISSR. Remote Sensing of Environment, 67, 1-14.

Price, J. C. (1984). Land surface measurements from the split window channels of the NOAA 7 Advanced Very High Resolution Radiometer. Journal of Geophysical Research, 89, 7231-7237.

Snyder, W., Wan, Z., Zhang, Y. and Feng, Y. (1998). Classification-based emissivity for land surface temperature measurement from space. International Journal of Remote Sensing, 19, 2753-2774.

Sobrino, J. A. and Raissouni N. (2000). Toward remote sensing methods for land cover dynamic monitoring: application to Morocco. International Journal of Remote Sensing, 21, 353-366.

Sobrino, J. A. and Romaguera, M. (2004). Land surface temperature retrieval from MSG1-SEVIRI data. Remote Sensing of Environment, 92, 247-254.

Takeuchi, W., Nemoto, T., Kaneko, T. and Yasuoka, Y. (2010). Development of MTSAT data processing, distribution and visualization system on WWW. Asian Journal of Geoinformatics, 10(3), 29-33.

Ulivieri, C., Castronuovo, M., Francioni, R. and Cardillo, A. (1994). A split window algorithm for estimating land surface temperature from space. Advances in Space Research, 14(3), 59-65.

Wan, Z. and Dozier, J. (1996). A generalized split-window algorithm for retrieving land-surface temperature from space. IEEE Transactions on Geoscience and Remote Sensing, 34(4), 892-905.

Wan, Z. (1999). MODIS Land-surface Temperature Algorithm Theoretical Basis Document.

Wan, Z., Zhang, Y., Zhang, Q. and Li, Z. (2002). Validation of the land-surface temperature products retrieved from Terra Moderate Resolution Imaging Spectroradiometer data. Remote Sensing of Environment, 83, 163-180.

Wan, Z. (2008). New refinements and validation of the MODIS land-surface temperature/emissivity products. Remote sensing of Environment, 112, 59-74.

Wan, Z. (2013). New refinements and validation of the collection-6 MODIS land-surface temperature/emissivity product. Remote sensing of Environment, 140, 36-45.